Proceedings of the International Conference on Aerospace Science and Technology
26 - 28 June 2008, Bangalore, India

INCAST 2008-057

DYNAMIC AND AEROELASTIC ANALYSIS OF A TRANSPORT AIRCRAFT

N.G. Vijaya Vittala[1], A.C.Pankaj[2], R.Swarnalatha[3]
[1] Structural Technologies Division, National Aerospace Laboratories, Bangalore, India, vittal@css.nal.res.in
[2] Structural Technologies Division, National Aerospace Laboratories, Bangalore, India acpankaj@css.nal.res.in
[3] Former Scientist, Structural Technologies Division, National Aerospace Laboratories, Bangalore.

ABSTRACT: The dynamic and aeroelastic characteristic of a transport aircraft has been established using MSC/NASTRAN. Correlation of the dynamic characteristics of the aircraft obtained from analysis with the Ground Vibration Test results of the aircraft is studied. The doublet lattice method has been used to estimate the appropriate unsteady air loads generated on the lifting surfaces of the aircraft. In an attempt to realize the realistic flutter margins, the analysis results of the aircraft for the control surfaces rotational modes have been tuned to the Ground Vibration Test results after establishing the first cut analysis results. Flutter analysis of the complete aircraft has been carried out by both PK and KE methods and the critical flutter velocities have been evaluated. The flutter margins for the aircraft are established with respect to the FAR 25 requirements. All the considered aircraft configurations have been found to satisfy the FAR 25 requirements and have been subsequently cleared from flutter criteria with substantial flutter margins.

1. INTRODUCTION

The interactions of a flexible structure with the aerodynamic forces acting on it are severe enough to influence the structural and aerodynamic design. The dynamic and aeroelastic analysis of an aircraft with main reference to its lifting and control surfaces is an essential aspect for finalization of the design cycle and is also required for obtaining flight clearance and certification of the aircraft. The paper explains the dynamic and flutter analysis carried out on the first prototype of SARAS. The aircraft is a twin turbo prop, multi-role, light transport aircraft having a cantilevered low wing and rear-fuselage mounted pusher engines. The landing gear is of retractable tri-cycle type configuration. It has a pressurised cabin, and is designed to have high cruise speed, high specific range and short take off and landing distances. Dynamic and flutter characteristics of the aircraft have been studied using MSC/NASTRAN.

The analyses were carried out for two configurations, corresponding to two fuel levels in the wing. For configuration-1, the fuel mass in each wing is 250 kg and for configuration-2, the fuel mass in each wing is 125 kg. It is essential that the flutter velocities and margins obtained by the analyses should satisfy the aeroelastic requirement as specified in FAR 25 to certify the aircraft.

2. FINITE ELEMENT MODEL

The fuselage, control surfaces, the stub wing and the stress- cleared model of the wing [1] have been used for the dynamic analysis. The finite element model was generated using Quad4 and Tria3 shell elements of MSC/NASTRAN [2]. The bolts at the attachment points are modeled by bar and rigid elements. Appropriate multipoint constraints have been applied to simulate the motion of control surfaces. Updation of the FE models was done for non-structural masses including the balance masses and the stiffness of the actuating mechanisms for the control surfaces. The individual FE models detailed above were checked for their mass and centre of gravity details and then integrated together to realize FE model of the full aircraft model (Fig.1) consisting of more than 6,72,000 degrees of freedom. The finite element model mass and centre of gravity are in close correlation with the design values (Table1).

Table 1 Mass and Centre of Gravity Details

Config.	Design Mass (kg)	X C.G (mm)	Y C.G (mm)	Z C.G (mm)	FEM Mass(Kg.)	X C.G (mm)	Y C.G (mm)	Z C.G (mm)
Config -1	5762.0	7916.39	0.0	0.0	5762.471	7916.584	-5.460718	-79.66621
Config-2	5512.0	7907.21	0.0	0.0	5512.471	7907.018	-5.708372	-37.61668

3. AERODYNAMIC MODEL

The right and left wing surfaces are each divided into four main zones corresponding to the main wing, inboard and outboard flaps and aileron. These zones are appropriately subdivided depending on the chord and span. In total the right half of the wing has two hundred and sixty-one boxes. Similarly the left half of the wing has two hundred and sixty-one boxes making a total of five hundred and twenty-two boxes. The horizontal tail is divided into three main surfaces corresponding to Horizontal Stabilizer, Elevator and Tabs. These surfaces are appropriately subdivided depending on chord and span. Horizontal tail in total has one hundred and seventy six boxes. The three surfaces of the vertical tail i.e., fin; rudder and tabs are suitably subdivided into trapezoidal boxes. Vertical tail in total has seventy-four boxes. The symmetric stub wing surfaces are each sub divided into trapezoidal boxes, chord wise four and span wise five and twenty in total.

The fuselage of the aircraft is modeled as a zy- slender body consisting of a series of elements having half-widths equal to the cross-sectional radii at each bulkhead station to ultimately realize the fuselage contour. To account for aerodynamic interference between panels and bodies, the interference tube is defined with its half-width equal to the maximum cross-sectional radius of the body (fuselage). The two nacelles are modeled as zy- slender bodies with slender body elements and interference elements. The interference elements have identical half-widths equal to the maximum nacelle radius. A beam spline is used to interpolate between aerodynamic and structural displacements for both fuselage and nacelles. The aerodynamic meshes described above are integrated thereafter to realize the aerodynamic model of the major individual components and the full aircraft (Fig.2). The interference between the body (fuselage) and the lifting surfaces wing, VT and stub wing is taken into consideration by declaring interference groups.

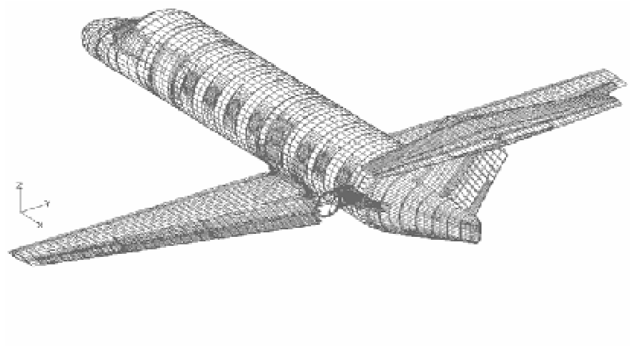

Fig.1 FE model of the aircraft

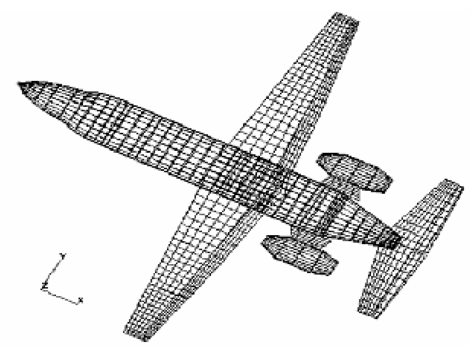

Fig.2 Aerodynamic model of the aircraft

4. ANALYSIS

Dynamic analysis of the free-free aircraft is carried out with no constraints at the wing attachment points. Appropriate condition for the nested position of flaps, hinge condition for the three control surfaces and respective control circuit stiffness have been applied to them at the actuation points for the initial analysis. In all the subsequent analyses the control surfaces stiffness were fine-tuned to realize the rotational mode of the elevator and rudder frequencies obtained through the ground vibration tests of the aircraft. The dynamic frequency spectrum of the complete aircraft has been obtained by invoking the Lanczos method in MSC/NASTRAN with unit mass criteria for normalizing the mode shapes. In the flutter solutions, full aircraft model was used and the eigen frequencies and modal vectors obtained from the eigen value solution of MSC/NASTRAN have been used. The flutter analysis of the aircraft is carried out after taking into consideration 45 modes, i.e. up to about 56 Hz of the spectrum [3, 4]. The cut off frequency includes rotational modes of the control surfaces, fuselage bending modes, wing bending modes and torsion modes, which are susceptible for flutter. The PK and KE methods have been used for the flutter analysis

5. RESULTS AND DISCUSSION

Table 2 compares the dynamic frequencies obtained through finite element dynamic analysis of the aircraft with ground vibration test results of the aircraft for configurations 1. Some typical mode shapes obtained from the analysis are presented in Fig 3 and Fig 4. The free-free analysis of the aircraft results in clear six rigid body modes followed by the elastic modes. The participation of the aft fuselage is seen in the occurrence of coupled modes. The wing bending and torsion modes are well separated. The major effect of presence of high HT in the T-Tail configuration is seen in the occurrence of HT bending and in-plane modes prior to VT lateral bending. Coupling of symmetric modes of lifting surfaces with longitudinal movement of fuselage is seen, as also that of anti-symmetric modes with the lateral movement. Fig 4 shows the VT longitudinal mode associated with HT symmetric bending and fuselage bending in the XZ-plane.

The results obtained for configuration-2 show the same trend with higher values in comparison to configuration-1. A good correlation between the analysis and experimental results are seen for both the configurations. The flutter results are tabulated in Table 3. The flutter plots for configuration 1 are shown in Fig.5. The VT longitudinal bending mode (Fig.4) coupled with Fuselage longitudinal bending and HT symmetric bending and elevator rotation leads to flutter. The flutter velocity (Vcr) and the flutter frequency obtained by PK method for the configuration-1 are 179.59 m/sec and 14.33 Hz. The corresponding values for the configuration-2 are 185.24 m/sec and 14.5 Hz.

Table 2 Dynamic Results of the Aircraft (Configuration-1)

Mode Remarks	GVT		FEM
	MIMO Freq (Hz)	Damping **(%)**	Freq (Hz)
Rigid Body Mode	2.15	6.81	0.118
Wing 1st ASym. B (FUS rot + HT Asym. B)	5.52	0.44	5.388
Wing 1st Sym. Bending	6.85	3.7	6.761
Fuselage bending (Wing Bending)	8.04	1.37	7.767
HT 1st Asym. Bending + VT Lateral Bending	11.53	0.84	11.40
Wing 2nd Asym. Bending	15.91	1.56	17.02
VT Longitudinal Bending	16.21	2.74	15.08
Wing 2nd Sym. Bending	16.82	1.83	23.19
VT Lateral B (Wing Asym.B + HT Asym. B)	17.37	4.54	19.03
HT 1st Sym. Bending	21.68	2.06	20.25
Fuselage longitudinal Bending	30.22	1.87	31.69

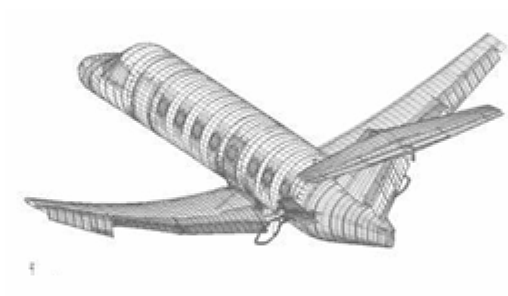

Fig.3 1st symmetric wing bending (6.76 Hz)

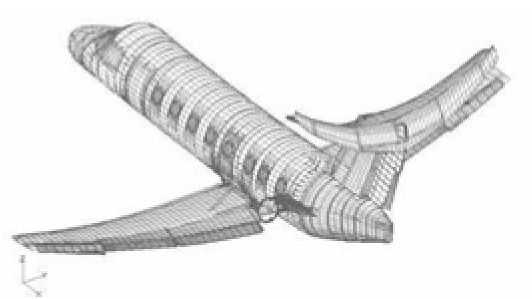

Fig.4 VT longitudinal and HT symmetric bending (15.08 Hz)

Table 3 Flutter Results of the Aircraft

Configuration	Method	Mode No	Flutter Velocity (Vf) (m/s)	Flutter frequency (Hz)	Flutter Margins (%)
1	PK	18	179.59	14.3359	27.76
	KE	18	179.68	14.3378	27.83
2	PK	18	185.24	14.5061	31.78
	KE	18	185.62	14.5046	32.05

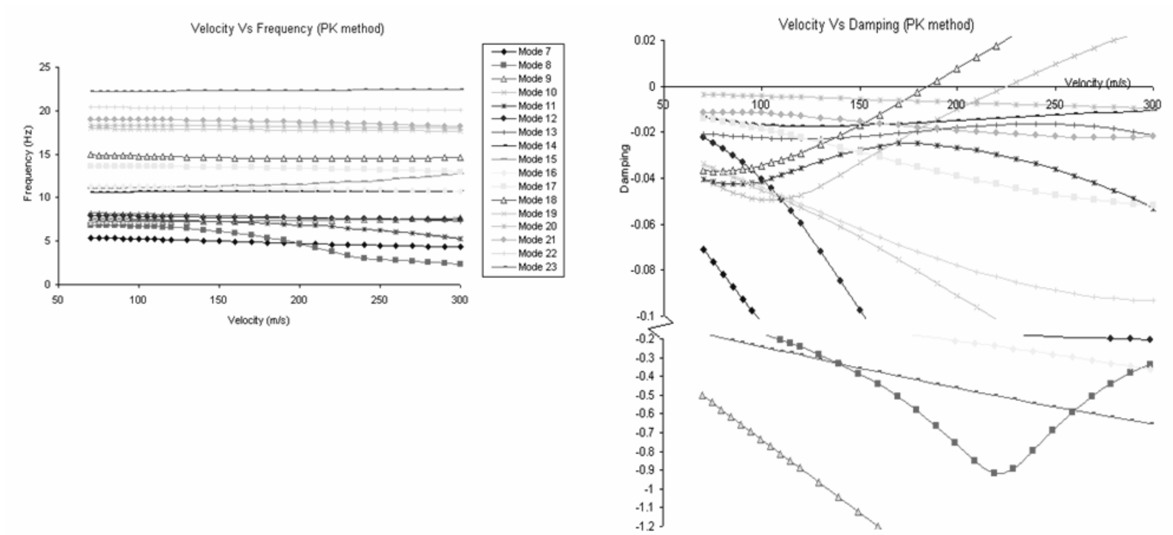

Fig.5 Flutter plots of the aircraft (configuration -1)

6. CONCLUSION

Good correlation between the analytical and experimental frequencies is observed. The flutter velocities obtained by PK and KE methods are consistent. The dive speed (*Vd*) of SARAS is 140.56 m/sec, (506 kmph) . FAR 25 [5] requires the flutter critical velocity to be 1.2 times the dive speed (*Vd*), which is 168.3 m/s. The value of $\left(\frac{V_f}{V_d}-1\right)$x100 gives the percentage of flutter margin that the aircraft has and this value should be greater than 20. The highT-tail design is a complicated configuration from the dynamic point of view, as the aft fuselage flexibility leads to coupled modes and results in plane modes accompanied by an out-of-plane motion of the tail structures. The flutter occurring in the 18th mode, is a coupled mode of VT longitudinal bending with HT symmetric bending with elevator rotation. The overall assessment of flutter summary given in Table 3 shows that the aircraft has a flutter margin of 27.76% for configuration 1 and 31.78% for configuration 2 against a requirement of 20% with respect to *Vd* satisfying the requirements of FAR 25.

ACKNOWLEDGEMENTS

The authors acknowledge all support received from colleagues of different groups in the laboratory and in particular the encouragement provided by the Head of the structures division and Director, NAL, Bangalore.

REFERENCES

[1] S Raja, R Swarnalatha, N.G.Vijaya Vittala, S Viswanath, GC Junjanna, KG Prashant, A Kiran Kumar, *Dynamic and Aeroelastic analysis of SARAS Empennage*, PD-ST-0323 (NAL, Bangalore, India),2003.

[2] MSC/NASTRAN Documentation (Msc Software Corporation, USA), 2005.

[3] N.G.Vijaya Vittala, R Swarnalatha, S Viswanath, A Kiran Kumar, *Dynamic and Aeroelastic analysis of SARAS Wing*, PD-ST-0322 (NAL, Bangalore, India),2003.

[4] N.G.Vijaya Vittala, R Swarnalatha, S Viswanath, A Kiran Kumar, *Dynamic and Flutter analysis of SARAS Aircraft*, PD-ST-0414 (NAL, Bangalore, India), 2004.

[5] FAR 25 Aviation Regulations, 2000.